

Pulsed Magnetic Field Measurements of the Composite Fermion Effective Mass

D.R. Leadley,¹ M. van der Burgt,¹ R.J. Nicholas,¹ C.T. Foxon² and J.J. Harris³

¹*Department of Physics, Oxford University, Clarendon Laboratory, Parks Road, Oxford, OX1 3PU, UK*

²*Department of Physics, Nottingham University, University Park, Nottingham, NG7 2RD, UK*

³*Department of Electronic Engineering, University College London. UK*

(Submitted to Phys. Rev. B May 11, 1995)

Abstract

Magnetotransport measurements of Composite Fermions (CF) are reported in 50 T pulsed magnetic fields. The CF effective mass is found to increase approximately linearly with the effective field B^* , in agreement with our earlier work at lower fields. For a B^* of 14 T it reaches $1.6m_e$, over 20 times the band edge electron mass. Data from all fractions are unified by the single parameter B^* for all the samples studied over a wide range of electron densities. The energy gap is found to increase like $\sqrt{B^*}$ at high fields.

73.40.Hm, 73.20.Dx, 72.20.Jv

The Fractional Quantum Hall Effect (FQHE) has been known for many years, [1] but a complete understanding has remained elusive due to the complex electron-electron interactions responsible. Recently a great deal of excitement was aroused by a model in which the electrons are transformed into Composite Fermions (CF). [2–7] In this model the Coulomb interaction of one electron with all the others is replaced with a Chern-Simons gauge field, equivalent to attaching an even number ($2m$) of flux quanta ($\Phi_0 = h/e$) to each electron. In a mean field approximation the gauge field exactly balances the external field at filling factor $\nu = 1/2m$ where the system of interacting electrons in high magnetic field is replaced by one of independent CFs in zero field. At other filling factors there are more (or less) flux quanta than required to cancel the gauge field and the CFs see an effective magnetic field, $B^* = B - 2m\Phi_0 n_e$. This leads to quantisation of the CF energy into Landau levels (LLs) and gaps open in exact analogy with the Integer Quantum Hall Effect (IQHE) of non-interacting electrons. Thus the FQHE may be simply regarded as the IQHE of Composite Fermions.

Several experiments have shown that CFs appear to behave like real particles, [4] in that they have a well defined Fermi wavevector and follow particle like trajectories under the influence of the effective magnetic field. Therefore it is of interest to know if an effective mass may be associated with these objects and what the origins of such a mass are. In an earlier work [5] (hereafter **I**) we treated the FQHE features in ρ_{xx} as Shubnikov-de Haas oscillations (SdHO) and analysed the temperature dependence of the amplitudes to determine the CF effective mass M^* for three samples of low electron density n_e . In this paper we report similar measurements for higher density samples in pulsed magnetic fields up to 50T, and observe a strong field dependence of M^* which is related to the electron-electron interactions. This report also presents both the highest electron density and the highest magnetic field at which the FQHE has been studied.

In our earlier work M^* was evaluated for each maximum and minimum between $\nu = 2/3$ and $1/3$, and found to be given by $M^* = (0.51 \pm 0.05) + (0.074 \pm 0.015)B^*$, in units of the free electron mass m_e . The same dependence was found for positive and negative values of B^* , i.e. for fractions above and below $\nu = 1/2$, and the mass values from samples with n_e differing by a factor of 2 was the same at a given value of B^* . This suggested that B^* , as opposed to the externally applied field B , was the important parameter and that the CF model was appropriate. For the samples studied in **I**, with n_e between 0.6 and $1.2 \times 10^{15} \text{m}^{-2}$, the maximum value of B^* accessed was 3.7T for the $\nu = 1/3$ minimum, at which point $M^* = 0.78m_e$. This is some 40% larger than measured at the lowest effective field of 0.5T for $5/9$. The experimental errors arising from uncertainty in the electron temperature and the fitting procedure are $\sim 0.1m_e$, however by now performing the experiment at higher effective fields we can test the dependence of M^* on B^* to a much greater degree. There has been much speculation as to what the mass does as $\nu = 1/2$ is approached, where the oscillations in ρ_{xx} are weak, with some reports of a strong divergence. [6] Our current data does not support this divergence, but in the present paper we restrict our analysis to regions where the oscillations in ρ_{xx} are reasonably large at low temperatures.

The measurements were performed on Hall bars of high quality GaAs-GaAlAs heterojunctions grown by MBE at Philips Research Laboratories. [8] Three samples (G627, G650, and G902) had significantly lower impurity contents due to the use of a short period AlAs/GaAs superlattice in the buffer layer. The samples were measured after photoexcitation to ensure maximum homogeneity and the largest possible features in the resistivity.

The relevant parameters of these samples as measured are given in Table 1 together with those for the samples reported in **I** for completeness.

The resistivity ρ_{xx} was measured for temperatures between 550mK and 4.2K using a ^3He cryostat in pulsed magnetic fields of up to 50T. The temperature was measured with a ruthenium oxide resistor mounted next to the sample. Good thermal equilibrium was ensured by keeping both the resistor and the sample immersed in ^3He liquid throughout the pulse. By comparing data obtained in the lower field section of the pulses, on both up and down sweeps, with data from the same samples studied in steady fields up to 16T, we estimate that the temperature rise during the pulse was less than 50mK. The current used was verified to be sufficiently low to prevent electron heating by comparing the peak amplitudes from shots taken with a range of currents. Induced voltages from the pulse were minimised by careful attention to the sample wiring and eliminated by averaging otherwise identical shots with opposite field directions. There is a slight shift in position of features between the two halves of the pulse due to an RC time constant which can be corrected for. Data taken as the field decays is generally better since the field is changing less rapidly and therefore we concentrate on this in the remainder of the paper.

Figure 1 shows the temperature evolution of the FQHE features for two of the samples studied. For sample G627, in Fig. 1(a), we see $\nu = 1/3$ at 38T and a well developed $2/7$ fraction at 45T, which is the highest field at which the FQHE has yet been observed. In Fig. 1(b) data is presented from the highest electron density sample yet studied, G902b with $\nu = 2/3$ at 30T. Taken together with our other data these figures show that FQHE states survive to very high magnetic fields in much the same form as at lower fields, but can now be observed at much higher temperatures. Similar data was obtained for samples G650 and G902a. However for sample G148 the resistance increased rapidly above 32T at low temperature as can be seen in Fig. 2. This means that of the features at fields above $\nu = 1/2$ only the $1/3$ minimum can be reliably analysed, although those below $1/2$ are unaffected. The onset of the rapid increase is near the $3/7$ fraction, but does not appear to be related to the filling factor. We ascribe this increase of resistance to magnetic field induced localisation since there is a greater background impurity concentration in sample G148. Unlike the G600 series of samples, it does not have a short period superlattice in the GaAs buffer layer. Similar dramatic increases in resistance have been seen around $1/3$ in GaAs hole gases, also having a large impurity content, which was ascribed to magnetically induced Wigner crystallisation. [9] However, in 2DEGs Wigner crystallisation is not thought to occur at filling factors greater than $1/3$ and so we do not believe these increases in resistance are due to any periodic arrangement of the electrons.

The oscillations in resistivity are described by the Ando formula [10]

$$\frac{\Delta\rho_{xx}}{\rho} \propto \frac{X}{\sinh X} \exp\left(-\frac{\pi}{\omega_c\tau_q}\right) \cos 2\pi(\nu - 1/2), \quad (1)$$

where $X = 2\pi^2k_B T/\hbar\omega_c$ and $\omega_c = eB/m^*$ is the cyclotron frequency. For Composite Fermions we replace B by B^* , ν by ν^* , m^* by M^* and τ_q by \mathcal{T}_q . From the temperature dependence of the oscillations a value of M^* can be obtained at each maximum and minimum, using the amplitude of the oscillation envelope and the effective field at which the extrema occur. Since Eq. (1) is valid for all fields, not just the FQHE minima, a value for M^* can be obtained at any field provided that data from the same measured B^* is used

at all temperatures. It is necessary to assume that \mathcal{T}_q (i.e. the level broadening) does not change with temperature over the region of interest. In the case of GaAs-GaAlAs electron gases at high fields we believe this to be a justifiable assumption. However, in cases where \mathcal{T}_q is not constant any mass values obtained must be treated with suspicion.

The analysis was performed on the FQHE features that are large at low temperature, i.e. we do not consider the weak features near to $\nu = 1/2$ where there are extremely large experimental uncertainties in the size of the oscillations and only a very limited temperature range where they can be distinguished from background noise. For each feature that we choose to analyse, only data for which $\Delta\rho/\rho < 50\%$ are considered, thus the FQHE features are always only a weak modulation of the conductivity and appear predominantly as sinusoidal oscillations periodic in $1/B^*$. For a feature at a given magnetic field this condition can always be satisfied by choosing a suitable temperature range. At lower temperatures the oscillations are less sinusoidal with the minima approaching zero resistivity and the positions of the maxima especially shifting from the expected field positions. Since the low temperature traces have the largest features the initial impression gained from Fig. 1 may be that these FQHE oscillations are not sinusoidal, but it should be remembered firstly that we are very careful only to analyse small oscillations and secondly that the usual electron SdHO show just the same behaviour. Higher harmonics can be included in Eq. (1) and we indeed find that $aX/\sinh X + b(X/\sinh X)^2$ fits both the electron and CF SdHO accurately up to $\Delta\rho/\rho \sim 90\%$, but that for small oscillations the extra term does not significantly alter the value of X deduced. Therefore to reduce the number of fitting parameters we have not pursued this approach in the analysis of this paper, choosing instead to limit the range of data considered. The derivation of Eq.(1) assumes a constant background resistance i.e. $\rho(B) = \rho(0)$ and shows how large a fraction of this background the oscillations are. However, for a sample like G148 where the features occur on a rising background it is necessary to consider the ratio $\Delta\rho/\rho(B)$ to obtain a good fit to Eq.(1), as opposed to just analysing the change in $\Delta\rho$ or $\Delta\rho/\rho(B = 0)$. The agreement with data from all the other samples justifies this approach, which we also used to analyse second generation CF features around $\nu = 1/4$ in **I**.

Figure 3 shows typical measured and fitted amplitudes for samples G650 and G902b. In each case the largest features are not included in the least squares fit to Eq. (1) at the lowest temperatures, where there are noticeable signs of saturation as the minima approach zero and our criterion is not satisfied. We find that Eq. (1) fits the data well over more than an order of magnitude change in $\Delta\rho$ and that it is very sensitive to the value of M^* . Therefore although there may be quite large errors in measuring the absolute sizes of the oscillations the experimental uncertainty in M^* is never more than $\pm 0.2m_e$ and for most cases is less than half this value.

The results of the analysis are shown in Fig. 4 as a function of n_e for several different fractions, including data from the samples of **I**. There is no unique n_e dependence covering all fractions, but it can be clearly seen that instead the mass values fall in pairs, corresponding to states with a common numerator p , e.g. $2/3$ and $2/5$. These have equal numbers of occupied CF Landau levels, but occur on either side of $\nu = 1/2$ with effective fields in opposite senses. This provides a simple demonstration of the symmetry of the states about $\nu = 1/2$ which is consistent with the CF model, rather than that of particle-hole conjugation where states of common denominator q (e.g. $1/3$ and $2/3$) look similar. In the low density

limit all states tend to the same effective mass, but the lower index CF Landau levels show an increasing “non-parabolicity”. By $n_e = 3 \times 10^{15} \text{m}^{-2}$ the effective masses for $\nu = 1/3$ and $\nu = 2/3$ differ by approximately 40%, while the masses for $\nu = 2/3$ and $\nu = 2/5$ differ by less than 5%. Furthermore the gradients of each line on Fig. 4 follow accurately a $1/p$ dependence. The CF mass may then be given by the expression

$$M^* = 0.510 + \frac{0.35}{p} n_e \quad (2)$$

in units of m_e , with n_e in units of 10^{15}m^{-2} . Since $B^* = \Phi_0 n_e / p$ this shows there is no additional dependence on n_e above that produced by the effective field.

Accordingly, M^* is shown as a function of the effective field in Fig. 5a, where data from a large number of different fractions and from samples with densities varying by an order of magnitude all lie on a single line. The best fit is shown by the dashed line,

$$M^* = (0.510 \pm 0.015) + (0.083 \pm 0.005)|B^*|. \quad (3)$$

Again in Fig. 5a, as in Fig. 4, there is no noticeable difference between data taken from either side of $\nu = 1/2$ showing that the sign of B^* is not important. (In the remainder of the paper B^* should be read as $|B^*|$). Taken together with our earlier data, we can now state that we have shown that there is a simple functional dependence of the CF mass on the single parameter B^* , covering more than a factor of 25 variation of B^* . At the highest effective field $M^* = 1.6m_e$, which represents an increase of $\sim 200\%$ over our range of B^* , and a factor of 24 enhancement over the GaAs band edge mass.

The measurement of M^* is equally a measurement of the CF cyclotron energy since

$$E_c^* = \hbar e B^* / M^*, \quad (4)$$

i.e. E_c^* is the separation of CF LLs. In fact it is the ratio kT/E_c^* (independent of B^*) that determines the oscillations in Eq. (1) so we could regard the energy gap as the more fundamental quantity, with M^* being a consequence of the model which considers CFs in an effective field. This E_c^* is equivalent to what would previously be known as the FQHE energy gap Δ , for a sample with infinitely narrow levels. However, unlike activation energy measurements which only give the separation between the extended state regions in adjacent LLs, this method directly probes the energy difference between the centers of the LLs and so the LL width does not need to be known. In Fig. 5b we show E_c^* as a function of the effective field for all the samples. With $B^* = 14\text{T}$ we see an energy gap of 12K for the 1/3 fraction, allowing FQHE features to be seen at quite high temperatures. It is again remarkable how plotting E_c^* against the effective field yields a single curve for all samples and all fractions considering both maxima, minima and either sense of B^* . By contrast Fig. 6, where the gap is plotted against the real field, shows no such orderly behaviour and many additional restrictions have to be added before a meaningful description of the data can emerge. (That the data points on Fig. 6 do not extend all the way along the dotted lines to $\nu = 1/2$ for each sample is a consequence of the ranges of field and temperature over which the FQHE may be observed.) Thus we make our claim that the Composite Fermion effective magnetic field is the single parameter that unifies all the experimental Fractional Quantum Hall Effect data.

Following this qualitative conclusion we wish to understand the functional dependence of E_c^* on B^* . The increase of M^* with B^* found in Eq. (3) necessarily means that E_c^* will show a sub-linear increase with effective field, as opposed to the linear increase that would be expected of a pure cyclotron energy for particles with a constant effective mass. The problem may be visualised in two ways: either (i) E^* is treated as a true CF cyclotron energy and we have to explain why the effective mass, as a property of real CF particles, increases with B^* ; or (ii) we explain how E_c^* , as the FQHE energy gap, increases with B^* and treat M^* as just a parameter defined via Eq. (4).

Taking the first approach, we recall that the measured single particle electron effective mass may increase slightly with electron density, since when the Fermi energy is higher the conduction band non-parabolicity becomes important and that this non-parabolicity can be accurately accounted for by the proximity of other conduction and valance bands. [11] For the normal low field SdHOs there is however no change of mass with field since all charge transport occurs at the Fermi energy which remains (approximately) constant as it moves between LLs. To account for the CF data presented here in terms of non-parabolicity the CF LLs would need to deviate a lot more from parabolic bands than is the case for the bare electrons and also the CFs responsible for conduction would have to come from much higher in the band as $|B^*|$ increased. Thus corrections to the mass from non-parabolicity seems unlikely to be the explanation.

Now we turn to the second case where the energy gap is considered first. The FQHE is the result of a many body Coulomb interaction and so theoretically the energy gap has been written as $\Delta = C_\nu e^2 / (4\pi\epsilon\epsilon_0 l_0)$, where l_0 is the cyclotron radius (proportional to the interparticle spacing) and C_ν is a fixed coefficient, different for each fraction. Halperin, Lee and Reed [3] (HLR) have used this relationship and argued on dimensional grounds that the high field limit of M^* should show a square root dependence on carrier density through l_0 . [12] This corresponds to a \sqrt{B} dependence for both the cyclotron energy and the mass for any given fraction. Since $B^* = B(1 - 2\nu)$ this approach also gives a $\sqrt{B^*}$ dependence, but only for each fraction separately. However our data clearly shows that although there is not a single functional dependence on n_e (and hence B) covering all fractions, if instead we use B^* there is a single dependence for all fractions and all densities. In this spirit the data of Fig. 5b has been fitted to $E_c^* = a\sqrt{B^*}$ as shown by the dashed line with $a = 3.3(\pm 0.2)\text{KT}^{-1/2}$. If the exponent of B^* is also allowed to vary the best fit is achieved for a power of 0.57, although if only the high field data ($B^* > 2\text{T}$) is considered the result is 0.51. Thus it seems that a $\sqrt{B^*}$ behavior adequately describes our data for the energy gap, at least at high fields

So is there a justification for a $\sqrt{B^*}$ dependence? The HLR dimensional argument can be rewritten in terms of the effective (CF) parameters. In particular this allows us to introduce the cyclotron radius of the composite particles. We write this as $l_0^* = \sqrt{\hbar/eB^*}$, which means we have effectively ignored the presence of all filled CF levels in determining the inter (composite) particle spacing. This is a reasonable assumption because the orthogonality of CF wavefunctions in different CF LLs means there will only be strong interactions between CFs of the same LL. Using this definition we have

$$E_c^* = C^* \frac{e^2}{4\pi\epsilon\epsilon_0 l_0^*} = C^* \frac{e^2}{4\pi\epsilon\epsilon_0} \sqrt{\frac{eB^*}{\hbar}} \quad (5)$$

where C^* is now the same constant for all fractions. Using Eq. (4) to define M^* we can also

write

$$M^* = \frac{4\pi\epsilon\epsilon_0}{C^*} \left(\frac{\hbar}{e}\right)^{3/2} \sqrt{B^*}. \quad (6)$$

So in the high field limit this dimensional argument gives a square root dependence on B^* of both the gap and the CF mass, with Eq. (5) predicting a gapless system at $\nu = 1/2$ as required. From the fit to Fig. 5b we have an experimental value of $C^* = 0.063 \pm 0.005$, valid for all fractions. C_ν has been calculated for finite systems [13] using Laughlin wavefunctions and the hierarchical model to be $C_{1/3}=0.102$; $C_{2/5}=0.063$; $C_{3/7}=0.049$ (although there are large uncertainties for the higher order fractions). Transforming to CF parameters by $C^* = \sqrt{2p+1}C_\nu$ results in a spread of values of $C^*=0.177$; 0.141; 0.130 respectively for the 1/3, 2/5 and 3/7 fractions. The finite 2DEG thickness will reduce the calculated values by approximately half and is a stronger effect at higher field which will reduce this spread. [14] However, this correction still leaves a small difference between experiment and theory, which cannot be attributed to the effects of level broadening since our measurements of E_c^* are from level center to center. Future calculations using wavefunctions appropriate to Composite Fermions may clarify the situation.

Below about 2T, in the region where the mass has become almost constant, the energy gap is smaller than predicted by the strict square root behaviour and by 0.5T there is almost a factor of 2 difference. This is more obvious in the plot of effective mass Fig. 5a, where the square root behaviour is shown as a dotted line. Below 2T the experimental mass values are considerably larger than the $\sqrt{B^*}$ behaviour. This could be interpreted as C^* tending towards zero as $\nu = 1/2$ is approached where the dimensional estimation is expected to break down, as it must at very low effective fields or M^* would become less than the single particle mass. Such a decrease in C^* would have the effect of allowing the gapless system to exist over a finite range of field either side of $\nu = 1/2$, but would not lead to a divergent mass as $B^* \rightarrow 0$ [6,7] unless $C^* \rightarrow 0$ faster than $\sqrt{B^*}$. Thus the upshot of this discussion is that while the high effective field data can be described quite well with a $\sqrt{B^*}$ dependence, this breaks down as $\nu = 1/2$ is approached where the dimensional argument fails and corrections to the mean field theory of CFs must be applied. In the low field region our original description of the data by Eq. (3) remains far more accurate, while still adequately describing the high field behaviour, so that from a purely empirical point of view the linearly increasing mass remains the most general description.

In conclusion we have measured values for the Composite Fermion effective mass in pulsed magnetic fields of up to 50T. M^* shows the same approximately linear increase with effective magnetic field that we found earlier at low fields and reaches a value of $1.6m_e$ for an effective field of 14T, achieved by placing $\nu = 1/3$ at 42T. We correspondingly find that the CF cyclotron energy increases sub-linearly with B^* and that a single $\sqrt{B^*}$ behaviour agrees very well with data from all the fractions with $B^* > 2T$. We have discussed some possible origins of this behaviour but in the absence of detailed CF energy level calculations can draw no definitive conclusions. The results presented here strongly support the Composite Fermion interpretation of the FQHE and show that the most significant parameter in determining the properties of the CF particles is the effective field B^* . This behaviour has only become clear by extending the study of CF properties to high densities using pulsed magnetic fields.

MvdB acknowledges support from the EC Human Capital and Mobility programme.

REFERENCES

- [1] D.C. Tsui, H.L. Stormer and A.C. Gossard, Phys. Rev. Lett. **48**, 1559 (1982); R.L. Willett *et al.*, *ibid.* **59**, 1776 (1987); J.R. Mallett *et al.*, Phys. Rev. B **38**, 2200 (1988) T. Chakraborty and P. Pietilainen, *The Fractional Quantum Hall Effect* (Springer-Verlag, New York, 1988)
- [2] J.K. Jain, Adv. Phys. **41**, 105 (1992)
- [3] B.I. Halperin, P.A. Lee and N. Reed, Phys. Rev. B **47**, 7312 (1993)
- [4] R.L. Willett *et al.*, Phys. Rev. Lett. **71**, 7344 (1993); W. Kang *et al.*, *ibid.* **71**, 3850 (1993); V.J. Goldman *et al.*, *ibid.* **72**, 2065 (1994)
- [5] D.R. Leadley, R.J. Nicholas, C.T. Foxon and J.J.Harris, Phys. Rev. Lett. **72**, 1906 (1994)
- [6] R.R. Du, H.L. Stormer, D.C. Tsui, A.S. Yeh, L.N. Pfeiffer and K.W. West, Phys. Rev. Lett. **73**, 3274 (1994)
- [7] H.C. Manoharan, M. Shayegan and S.J. Klepper, Phys. Rev. Lett. **73**, 3270 (1994)
- [8] C.T. Foxon, J.J. Harris, D. Hilton, J. Hewett and C. Roberts, Semicond. Sci. Tech. **4**, 582 (1989)
- [9] M.B. Santos, J. Jo, Y.W. Suen, L.W. Engel and M. Shayegan, Phys. Rev. B **46**, 13639 (1992)
- [10] T. Ando, J. Phys. Soc. Jpn. **37**, 1233 (1974)
- [11] M.A. Hopkins, R.J. Nicholas, P. Pfeffer, W. Zawadzki, D. Gauthier, J.C. Portal and M.A. DiForte-Poisson, Semicond. Sci. Tech. **2**, 568 (1987)
- [12] As HLR evaluate l_0 at $\nu = 1/2$ but use $C_{1/3}$ their value for M^* is ambiguous.
- [13] N. d'Ambrumenil and R. Morf, Phys. Rev. B **40**, 6108 (1989)
- [14] F.C. Zhang and S. Das Sarma, Phys. Rev. B **33**, 2903 (1986)

FIGURES

FIG. 1. Resistivity of (a) sample G627, and (b) G902b, at temperatures between 0.6 and 2.2K, showing FQHE features at the highest fields yet observed.

FIG. 2. Resistivity of sample G148, showing a rapid increase in resistivity above 32T at low temperatures.

FIG. 3. Temperature dependence of the resistivity oscillations of (a) sample G650, and (b) G902b, with the fits to the Ando formula shown by dashed lines.

FIG. 4. The Composite Fermion effective mass M^* deduced for the maxima and minima of the resistivity oscillations shown as a function of carrier density n_e for each fraction p/q . The fitted lines have gradients $\propto 1/p$.

FIG. 5. (a) CF effective mass and (b) CF energy gap as a function of the effective field B^* . The fitted lines are described in the text.

FIG. 6. E_c^* plotted as a function of the external field B showing how this does not lead to the simple dependence found in Fig. 5b where B^* is the independent variable. The lines connect the data to $\nu = 1/2$ for each sample.

TABLES

TABLE I. Sample parameters

Sample	Spacer Layer Å	Electron Density 10^{15}m^{-2}	Mobility m^2/Vs
G902a	200	4.50	160
G902b	200	4.84	180
G148	400	3.26	220
G627	400	3.05	370
G650	800	2.26	630
G640	1200	1.17	680
G641	1600	0.90	400
G646	2400	0.63	200

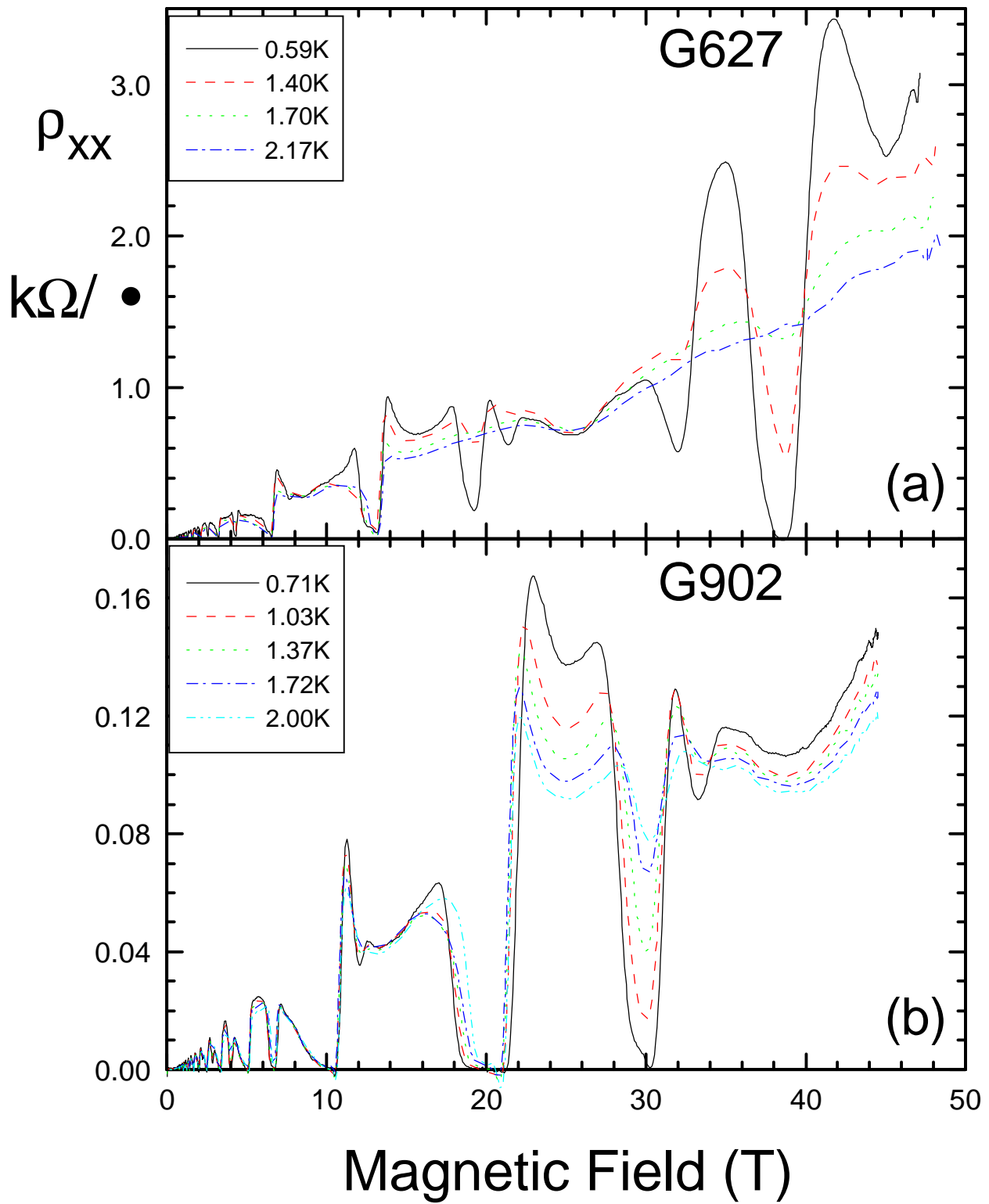


Fig. 1

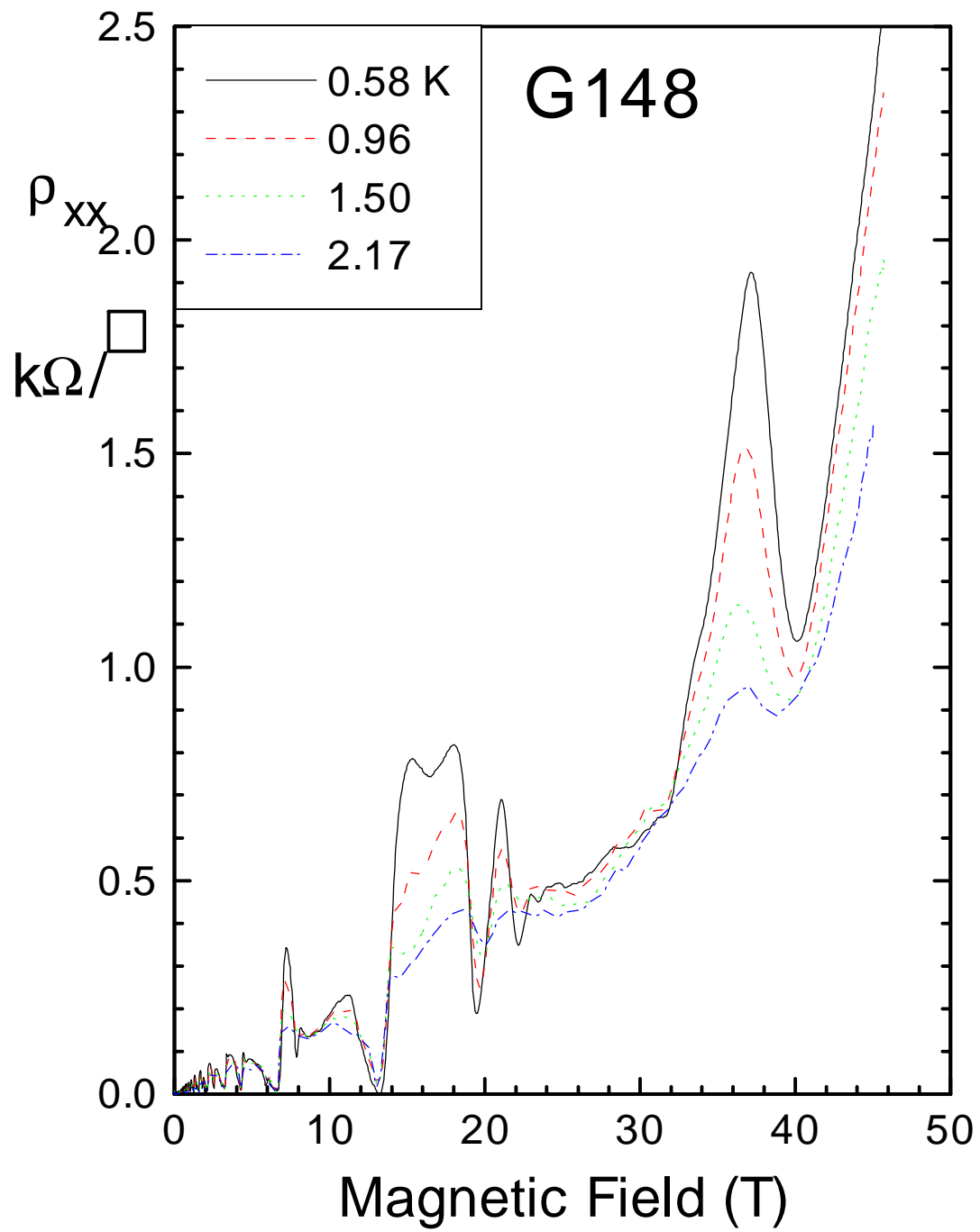


Fig.2

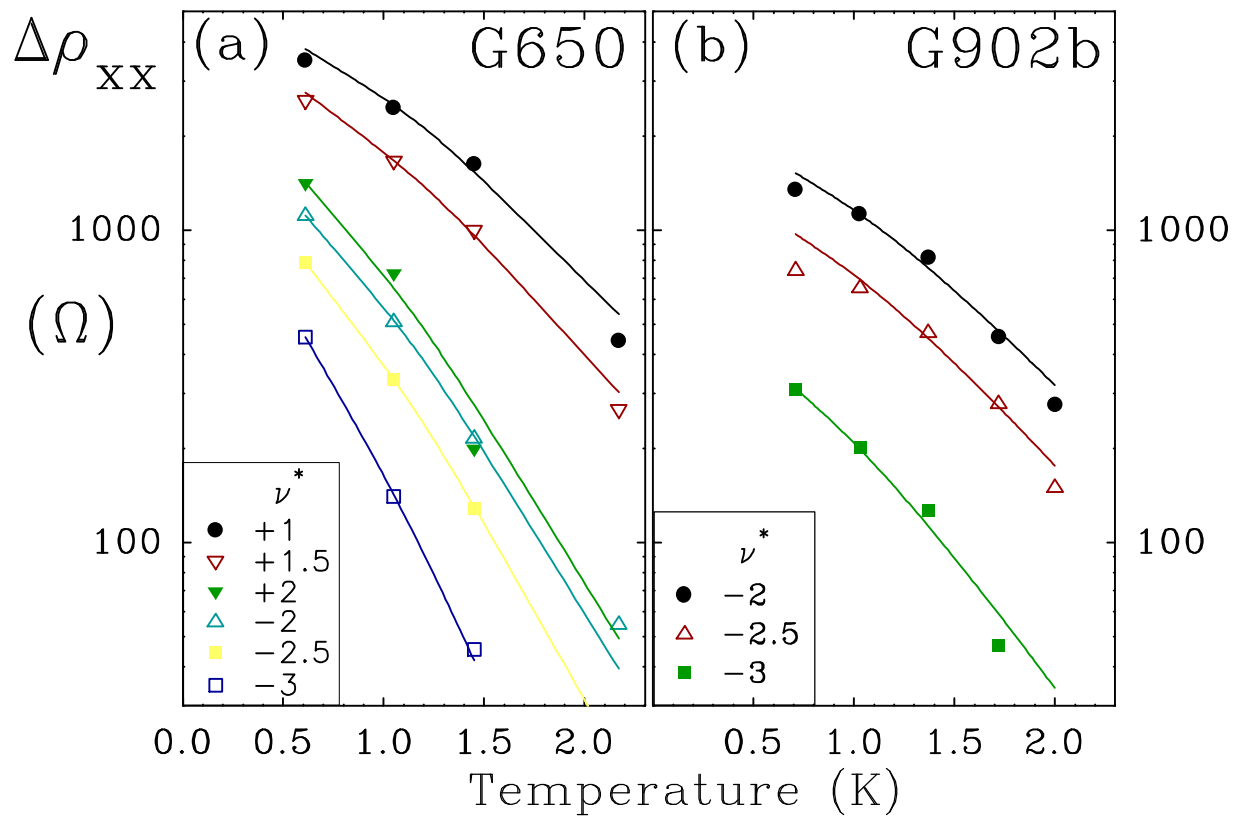


Fig. 3

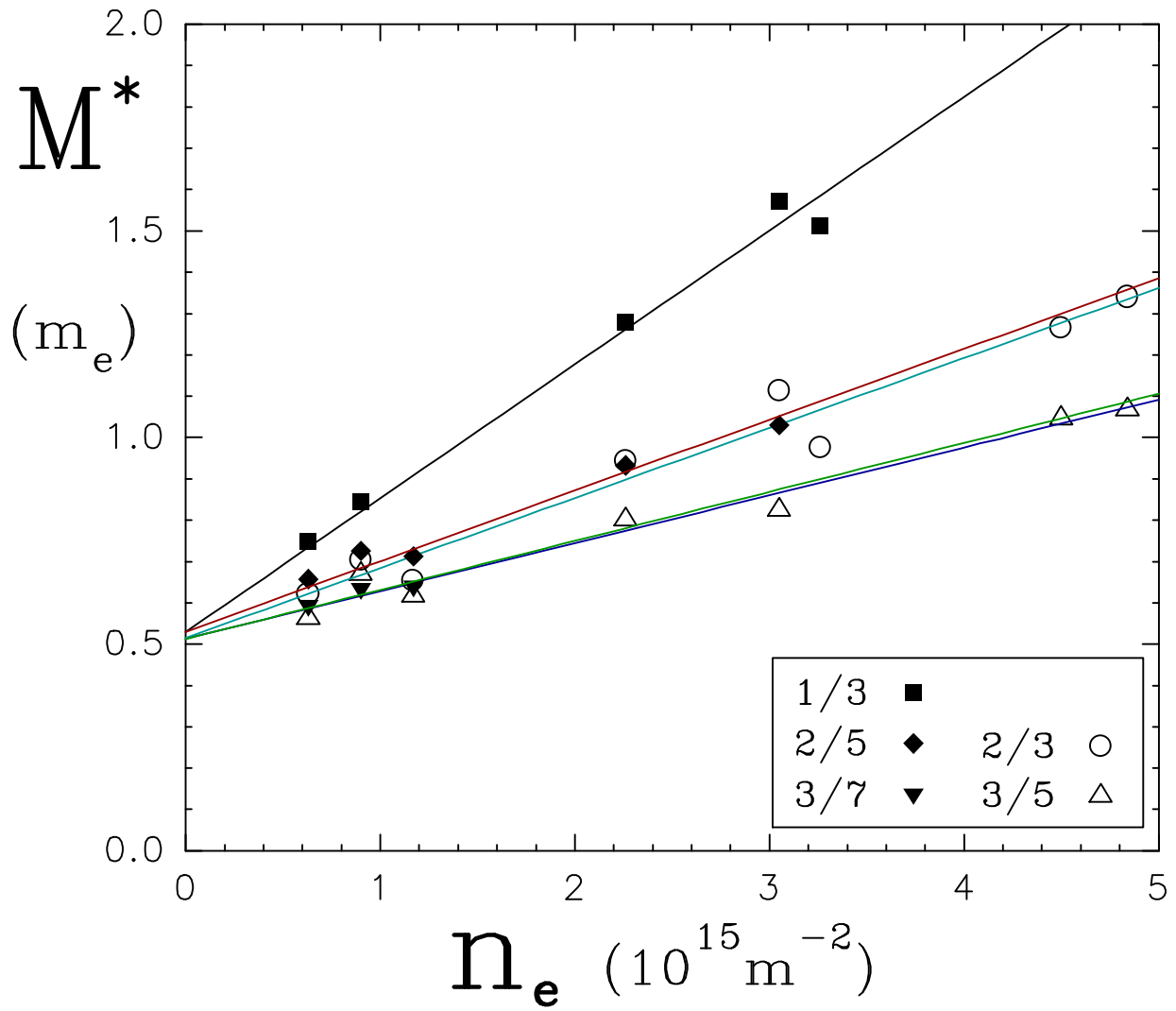


Fig 4

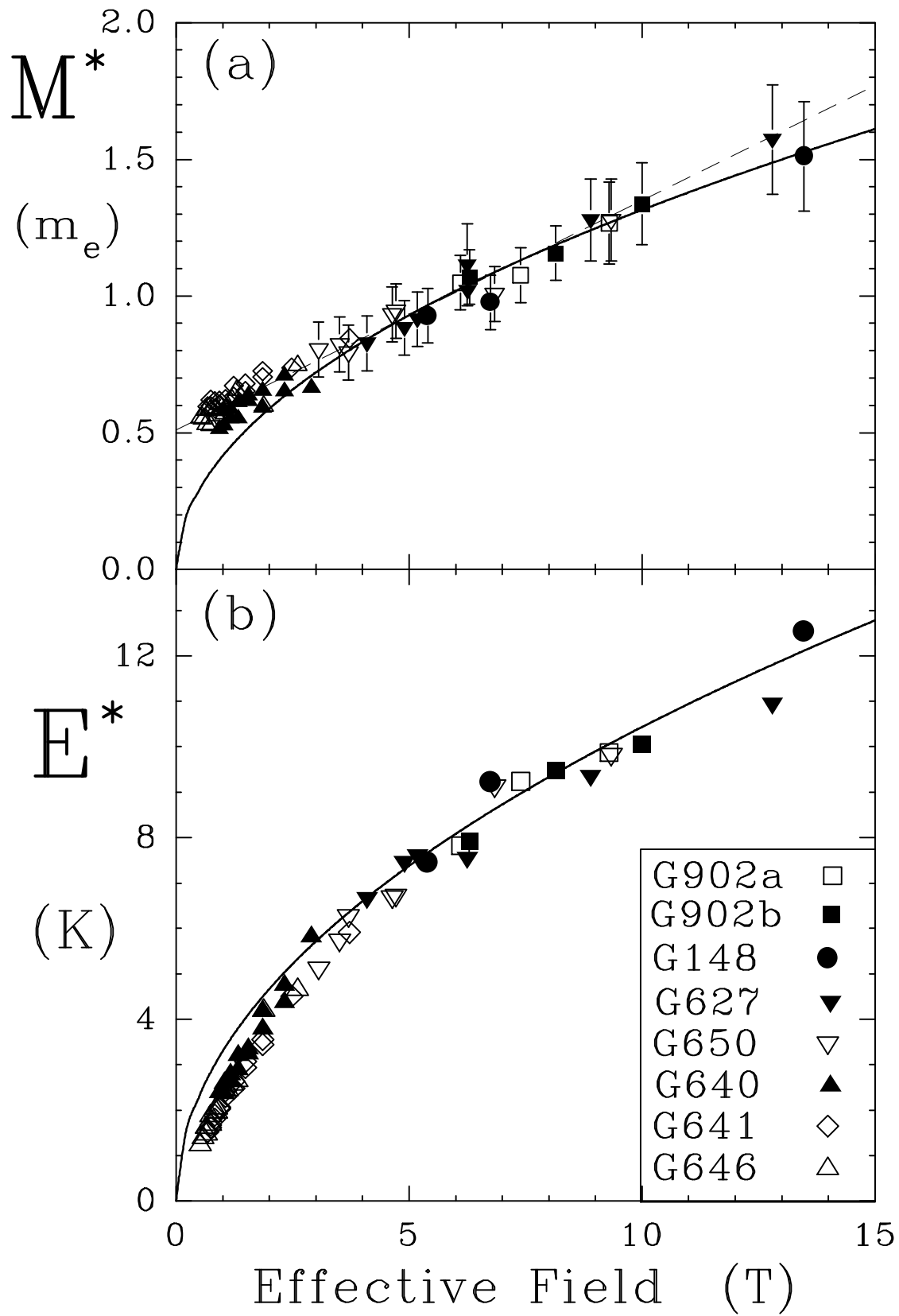


Fig 5

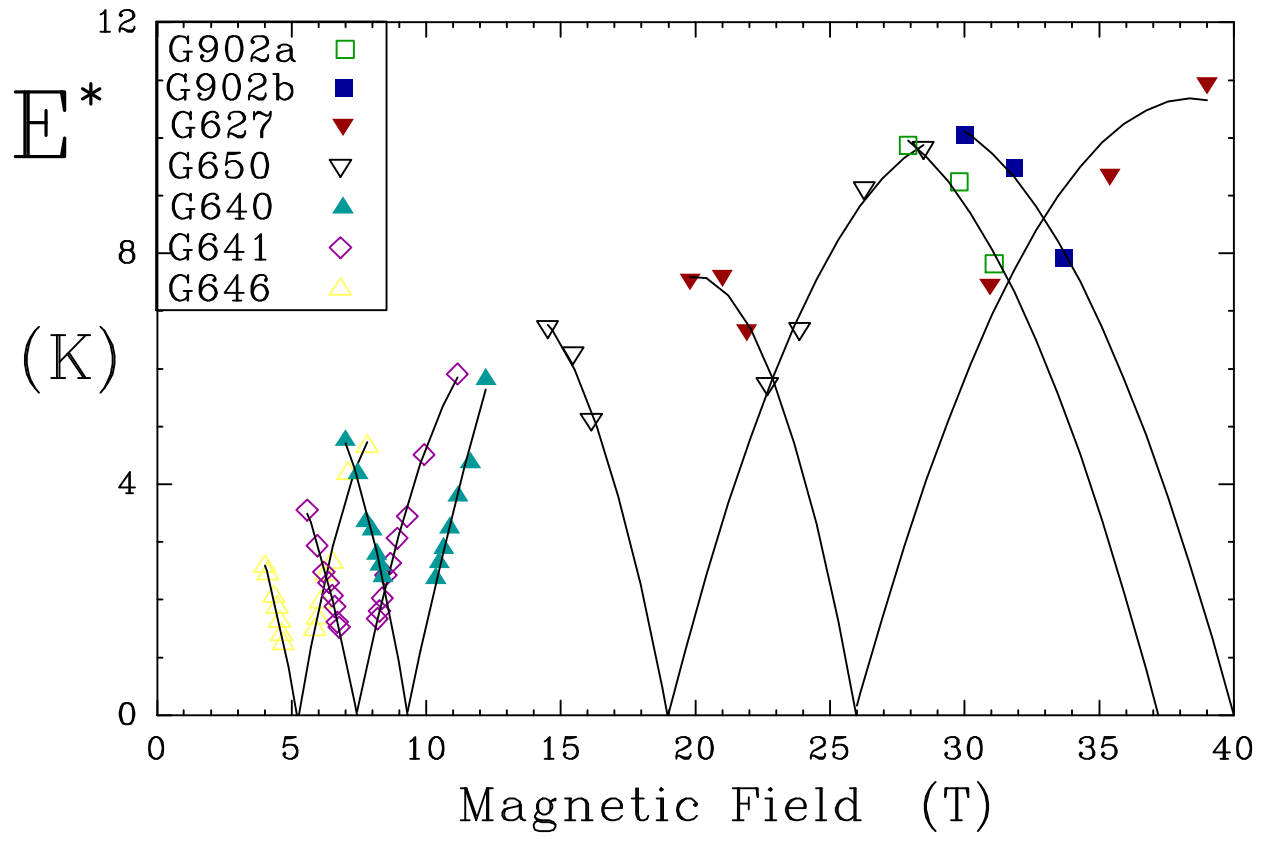


Fig 6